Performance Assessment of 40 Gb/s Burst Optical Clock Recovery Based on Quantum Dash Laser

Jun Luo, Josué Parra-Cetina, Pascal Landais,
Harm J. S. Dorren, and Nicola Calabretta

We report a 40 Gb/s burst mode optical clock recovery (BM-OCR) by injection locking a dynamically switched quantum dash mode-locked laser diode. We investigated in detail the performance of the BM-OCR operation after 52 km transmission. High quality BM-OCR after transmission is achieved with a locking time of ∼25 ns, and 40 GHz recovered packet clock with 46 dB signal to noise floor suppression and 64 fs timing jitter (100 Hz to 1 MHz). The reported BM-OCR has a continuous tuning wavelength range from 1535 to 1560 nm, power dynamic range of no less than 6.7 dB. The frequency deviation tolerance of the BM-OCR is within −427 to +226 ppm at 39.813 Gb/s (OC-768 standard line rate), which is compliant with the specifications in the IEEE 40/100-Gb/s Ethernet standard. These results indicate the promising future applications of the proposed BM-OCR in high speed burst mode optical receiver.

Optical receiver, optical clock recovery, quantum dash/dot, semiconductor device, injection locking.

I. Introduction

IN FUTURE high capacity optical telecom and datacom networks, burst mode optical receivers are demanded to handle bursty data traffic at bit rates beyond 40 Gb/s. Burst mode optical clock recovery (BM-OCR) is one of the key functionalities of such receivers. For practical implementation, the following important issues of a BM-OCR have to be considered. Firstly, fast locking/unlocking operation is required for a BM-OCR. Considering 40 Gb/s packets with typically 1500 bytes, the payload duration is ∼300 ns with the guard times of few tens of ns to optimize the traffic load. This requires BM-OCR with locking/unlocking times in the order of few tens of ns to enable high bit rates burst data reception. Secondly, the tolerance to timing jitter of the recovered clock becomes more stringent as the data rate increases (e.g. timing jitter <4.5 ps is required for OC-768 [1]). Thirdly, performance of the BM-OCR such as the wavelength operation range, the power dynamic range, and the frequency deviation tolerance need to be investigated in order to meet the requirements of practical application. Furthermore, small footprint, low power consumption, and low cost should be taken into account.

Current optical clock recovery (OCR) systems for high bit rates data is usually implemented by using optical phase-locked loop (OPLL) [2] or passive optical periodical filters [3], [4]. The OPLL approach results in a long locking time of a few microseconds in order to achieve a low timing jitter, which is unacceptable for burst mode operation. On the other hand, BM-OCR based on passive optical periodical filters is able to achieve fast locking/unlocking time (a few ns), but it requires precise signal wavelength alignment to match the optical periodical filter. This makes it less attractive in the practical application. Moreover, extra amplification is usually required due to the lossy passive elements leading to a bulky system. Recently, OCR based on injection locking of quantum dash mode-locked laser diodes (QD-MLLD) has been extensively investigated and characterized [5]-[7]. Thanks to the extremely narrow mode-beating spectral linewidth (<50 kHz) [7], the OCR based on QD-MLLD is able to produce very low timing jitter clock (<100fs) [6]. Moreover, the potential of exploiting the QD-MLLD as BM-OCR has been investigated in [8], and for the first time a 40 Gb/s BM-OCR operation has been demonstrated in [9].

In this letter, we further investigated in detail the operation and performance of the BM-OCR enabled by QD-MLLD with 40 Gb/s packets transmitted over 52 km fiber link. We achieved 40 Gb/s BM-OCR operation after transmission with locking time of ∼25ns, and high quality packet 40 GHz clock of 46 dB signal to noise floor suppression, and 64 fs timing jitter (100 Hz to 1 MHz). Our performance evaluation results show that high quality OCR is able to be achieved with continuous tuning wavelength range from 1535 nm to 1560 nm, power dynamic range of no less than 6.7 dB, and frequency deviation tolerance within – 427 ppm to +226 ppm at OC-768 standard line rate. This is sufficient to meet the specifications in the IEEE 40/100-Gbps Ethernet standard.

II. Burst Mode OCR Operation

The experimental setup to assess the performance of the QD-MLLD enabled 40 Gb/s BM-OCR after transmission is depicted in Fig. 1. SHF RZ-OOK transmitter module (SHF46210C) is used to produce the 39.813 Gb/s (OC-768 standard line rate) RZ-OOK packets. The optical packets are centered at 1550.3 nm with a payload duration length of 286 ns (consisting of multiple of 2^7-1 PRBS patterns) and a guard time of 45 ns. The PRBS pattern length is limited by the

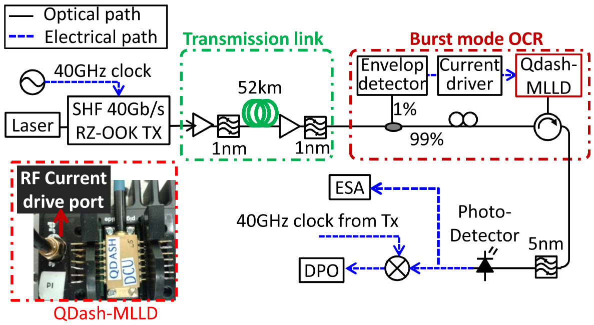

Fig. 1. Experiment setup of burst mode OCR based on QD-MLLD. ESA: electrical spectrum analyzer, Qdash-MLLD: quantum dash mode-locked laser diode, DPO: real time digital sampling oscilloscope.

payload duration, OCR based on QD-MLLD with higher order PRBS pattern ($2^{31}-1$ PRBS) is also feasible [7]. The 40 Gb/s packets are amplified to 12 dBm and launched into 52 km dispersion compensated fiber link. After the transmission, the optical packets are amplified and fed into the BM-OCR.

At the input of the BM-OCR, the 40 Gb/s data packets are split with 99:1 power splitting ratio. The 1% part is detected by a low speed optical receiver (622 Mb/s optical receiver) as the envelop detector to extract the packet envelop while the 99% part is sent to injection lock the QD-MLLD. The QD-MLLD employed as BM-OCR is butterfly packaged (see the inset of Fig. 1), and has an 18 mA bias current threshold. It features over 12 nm multimode lasing spectrum centered at 1528 nm when operated at 20.5 °C. Although this device is polarization sensitive, polarization insensitive OCR using QD-MLLD has been demonstrated in [10]. The detected packet envelop signal operates as a control signal to dynamically switch on/off a current source that drives the QD-MLLD. Due to the lack of the proper current source, a 400 MSa/s arbitrary waveform generator (AWG) is used in this experiment. The AWG is externally triggered by the packet envelop signal. It produces a square gating current with peak current of 82 mA, and the same duration length as the data packets. Therefore when data packets are present, the packets envelop triggers the AWG output to power up the QD-MLLD. The injected 40 Gb/s RZ-OOK data forces the QD-MLLD to lock to the signal data rate via four-wave-mixing (FWM) in the resonant cavity [11], generating a 40 GHz synchronized clock. While the data packet is absent, the QD-MLLD is instantly switched off without any optical power output. Thus, the packetized clock is recovered by injection locking the QD-MLLD that is dynamically switched by the packet envelope.

At the output of the BM-OCR, the 40 GHz clock is selected out by a 5 nm optical filter and detected by a 40 GHz photodetector. The quality of the recovered clock is analyzed by the electrical spectrum analyzer (ESA) and further evaluated by mixing the recovered clock with the 40 GHz clock at the source. Time trace after mixing is acquired afterwards by using 1.25 GSa/s a real time digital sampling scope (DPO).

III. Experimental Demonstration

We first verified the performance of the proposed BM-OCR operating with a back-to-back 40 Gb/s packets. Fig. 2(a) shows

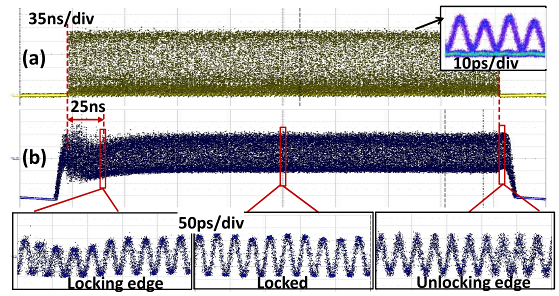

Fig. 2. (a) Time trace of the 40 Gb/s RZ-OOK packet that is injected into the QD-MLLD, inset is the corresponding eye diagram; (b) time trace of the recovered 40 GHz packetized clock, insets are the clock time trace at locking edge, locked region, and the unlocking edge respectively.

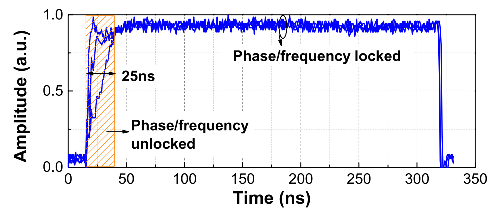

Fig. 3. Time trace results while mixing the recovered clock with the original 40 GHz clock from the transmitter side.

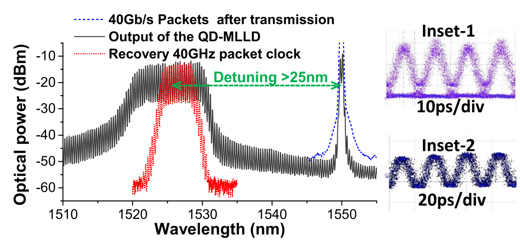

Fig. 4. Optical spectrum while externally injection locking of the QD-MLLD with the 40 Gb/s RZ-OOK packets after 52 km transmission; insets show the eye diagram of the 40 Gb/s packets after 52 km transmission (inset-1) and the waveform of the recovered packetized clock (inset-2).

the injection of 40 Gb/s optical packets with optical power of 4 dBm, and extinction ratio (ER) of 11 dB. Fig. 2(b) presents the time domain traces of the recovered 40 GHz packet clock. The insets show the magnification of the recovered clock at the different time position. Fig. 2(b) shows that ∼25 ns is required to lock the QD-MLLD and to produce a synchronized clock, while it unlocks instantly once the data burst is off. Fig. 3 shows the time trace after mixing the recovered clock with the original 40 GHz clock. These traces acquired by the DPO are shown by overlapping them in one packet period. The results confirm that ∼25 ns are needed to build up the frequency locking of the QD-MLLD, while the flat curve indicates that the recovered clock holds the locked frequency. These traces also indicate that the recovered packet clock starts randomly within the 25 ns build up time. Extra phase alignment between the packet clock and data packet will be required in practical operation.

We then investigated the performance of BM-OCR with 40 Gb/s data packets after 52 km transmission. Fig. 4 shows the optical spectrum of the 40 Gb/s packets after transmission (blue dash traces), the output of the QD-MLLD after injection locking (black solid traces), and the recovered packet clock (red dot traces). The insets also present the eye diagram of the

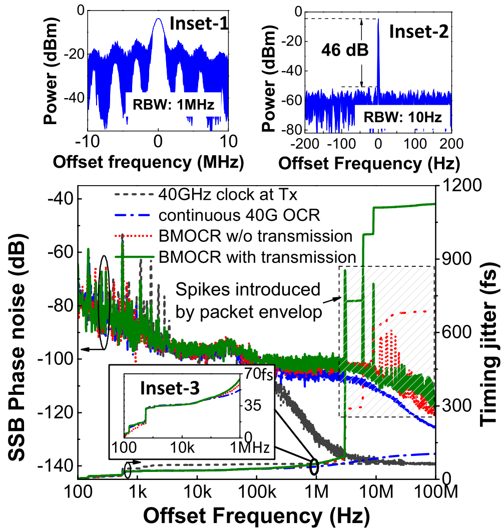

Fig. 5. SSB phase noise and timing jitter of the recovered packetized clock; insets show the electrical spectrum of the recovered clock with frequency span of 20 MHz (inset-1) and 400 Hz (inset-2). Inset-3 shows the timing jitter performance with frequency range from 100 Hz to 1 MHz.

packets and the waveform of the recovered clock. The packets after transmission have a 10 dB extinction ratio (ER). Signal quality is slightly degraded due to the extra amplitude noise and timing jitter introduced during the transmission. Note that the wavelength of injection packets is detuned over 25 nm to QD-MLLD lasing modes.

The quality of the 40 GHz packet clock is assessed in an electrical spectrum analyzer. Inset-1 and Inset-2 of Fig. 5 show the electrical spectrum of the recovered packet clock in 20 MHz and 400 Hz span respectively. The side modes shown in Inset-1 are due to the packetized envelop of the clock. Inset-2 shows that the clock tone has a signal-to-noise floor suppression ratio of 46 dB. Single side band (SSB) phase noise traces of 40 GHz clock at the transmitter (black dash), and OCR with continuous 40 Gb/s RZ-OOK data stream (blue dash dot), BM-OCR without (red dot) and with transmission (green solid) are shown in Fig. 5. The phase noise traces in Fig. 5 indicates negligible introduction of extra phase noise in the cases without and with 52 km transmission. Note that the frequency spikes located $>$3 MHz are due to the packetized envelop of the clock. Therefore phase noise integration $>$3MHz will produce a miss-leading timing jitter value. Herein, we assessed timing jitter by integrating the phase noise trace from 100 Hz to 1 MHz (see Inset-3 of Fig. 5) according to the method reported in [12], giving timing jitters of 59 fs and 64 fs in BM-OCR without and with transmission, respectively. Compared to the OCR case with continuous data (52 fs), there is an extra timing jitter of 7 fs and 12 fs. Furthermore, the SSB phase noise traces of BMOCR operation are almost overlapped within the frequency range from 100 Hz comparing with the trace of continuous 40G OCR. This indicates that the continuous OCR operation can give a good estimation of the phase noise and timing jitter performance (in the range of 100 Hz to 1 MHz) in BMOCR operation. Note that BMOCR without and with transmission integrating timing jitter between 100 Hz and 100 MHz are 0.64 ps and 1.1 ps, respectively, which are within the ITU standard ($<$4.5 ps).

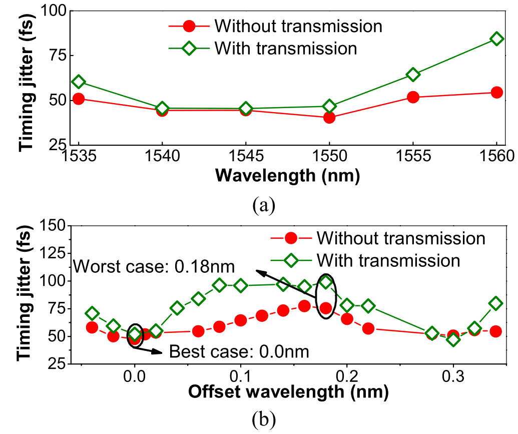

Fig. 6. Signal wavelength range of the OCR based on QD-MLLD: (a) timing jitter with signal wavelength coarsely tuned (5 nm/step); (b) timing jitter with offset wavelength tuned with respect to 1550.3 nm (0.02 nm/step).

IV. Performance Assessment

We further evaluated the performance of the QD-MLLD enabled OCR in terms of wavelength operation range, power dynamic range, and frequency deviation tolerance range. The setup and operation conditions are the same as in Section III. Note that in Fig. 5, we show that the burst mode operation introduces little extra phase noise to the recovered clock compared to the continuous OCR case within frequency range from 100 Hz to 1 MHz. Hence, continuous 40 Gb/s OOK signal is used in the following assessments. The timing jitter reported is integrated within the frequency range from 100 Hz to 1 MHz.

A. Wavelength Operation Range

Firstly, the signal wavelength operation range and wavelength dependence of the OCR is investigated using the injection signal at 39.813 Gb/s with optical power of 4 dBm. Fig. 6(a) shows the results with coarse wavelength tuning (5 nm/step) without and with transmission. High quality 40 GHz clock with timing jitter $<$100 fs is able to be recovered within the range from 1535 nm to 1560 nm. The transmission link introduces little distortion to the timing jitter performance. Fig. 6(b) shows the wavelength dependence while the injection signal wavelength is detuned finely in 0.02 nm steps with respect to 1550.3 nm. Like the results in Fig. 6(a), the timing jitter performance is similar without and with transmission link. Optimal injection signal wavelength is observed with the lowest timing jitter of $\sim$50 fs (0 nm and 0.32 nm is favorable offset wavelength). The optimal wavelength repeats approximately every 0.32 nm (about one free spectrum range of the QD-MLLD with 1 mm long cavity), which is due to the resonance instincts of QD-MLLD. A high quality clock is obtained with the worst timing jitter of 97 fs at the offset wavelength of 0.18 nm. These results indicate that the signal wavelength is able to be continuously tuned over the wavelength range from 1535 nm to 1560 nm without precise wavelength alignment. This is advantageous over the OCR scheme reported in [3], [4]. Furthermore, with little dependence of the input wavelength, the OCR is expected

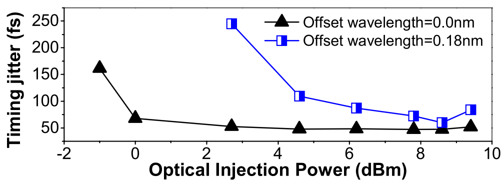

Fig. 7. Power dynamic range of the OCR at the best and worst signal wavelength detuning case.

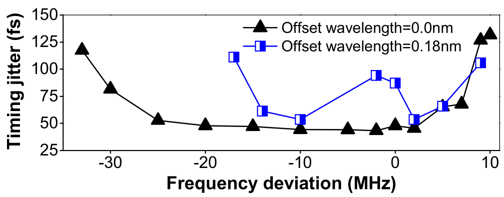

Fig. 8. Frequency deviation tolerance range of the OCR at the best and worst signal wavelength detuning case.

to work with packets while input wavelengths are varying at different time slots.

B. Power Dynamic Range

Secondly, with injection signal operated at bit rates of 39.813 Gb/s, the signal power dynamic range of the OCR is investigated after transmission at the best (1550.3nm, 0 nm offset wavelength to 1550.3 nm) and the worst (1550.48nm, 0.18 nm offset wavelength to 1550.3 nm) signal wavelength detuning case. As it is shown in Fig. 7, in the best wavelength detuning case, OCR is achieved with an injection power dynamic range of 11.6 dB (from −1 dBm to 9.6 dBm). While in the worst wavelength detuning case, the power dynamic range is decreased to 6.7 dB (2.7 dBm to 9.4 dBm) with recovered clock timing jitter of less than 250 fs. This means there is a 6.7 dB tolerable input signal power fluctuation range.

C. Frequency Deviation Tolerance Range

In practical implementation, signal data rates may vary due to the different transmitters in the networks. It is therefore important to investigate the frequency deviation tolerance range of the proposed OCR. Fig. 8 shows the results of frequency deviation tolerance range assessment of the OCR at the best and the worst signal wavelength cases while the injection signal power is fixed at 4 dBm. Timing jitter performance is assessed while detuning the bit rate of the injection signal to the reference bit rate of 39.813 Gb/s (OC-768 line rate). The results show that in the best wavelength detuning case, 40 GHz clock with timing jitter <130 fs is able to be obtained within the frequency deviation range from −33 MHz to +10 MHz. This corresponds to a clock frequency deviation tolerance within −829 ppm to + 250 ppm at OC-768 line rate. While in the worst wavelength detuning case, the frequency deviation range is within −17 MHz to 9 MHz with timing jitter less than 110 fs, corresponding to a clock frequency deviation tolerance within – 427 ppm to + 226 ppm at OC-768 line rate. The clock frequency deviation tolerance of the QD-MLLD based OCR is compliant with the IEEE 40/100-Gbps Ethernet specifications (+/−100ppm).

V. Conclusion

We demonstrated 40 Gb/s BM-OCR operation after 52 km transmission by injection locking a dynamically switched QD-MLLD, with locking time of ∼25 ns, and high quality 40 GHz packet clock with 46 dB signal to noise floor suppression, 64 fs timing jitter (100 Hz to 1 MHz). We investigated in detail the wavelength operation range, power dynamic range, and frequency deviation tolerance range of the proposed BM-OCR. We show that high quality low timing jitter OCR is achieved with continuous wavelength tuning range from 1535 nm to 1560 nm (covering almost the entire C-band), power dynamic range of no less than 6.7 dB with the worst wavelength detuning after 52 km transmission. Moreover, the frequency deviation tolerance of the BM-COR is within −427 ppm to +226 ppm, which is sufficient to meet the specifications in the IEEE 40/100-Gbps Ethernet standard. It should be pointed that the BM-OCR exploits a single integrated device (QD-MLLD) with low driving current, which leads to the advantage of compact footprint, operation simplicity and low power consumption.

References

[1] "The control of jitter and wander in the optical transport network," ITU-T, Recommendation G.8251, Sep. 2010.

[2] H. C. H. Mulvad, E. Tangdiongga, H. De Waardt, and H. J. S. Dorren, "40 GHz clock recovery from 640 Gbit/s OTDM signal using SOA-based phase comparator," *Electron. Lett.*, vol. 44, no. 2, pp. 146–147, 2008.

[3] D. Petrantonakis, G. T. Kanellos, P. Zakynthinos, N. Pleros, D. Apostolopoulos, and H. Avramopoulos, "A 40 Gb/s 3R burst-mode receiver with 4 integrated MZI switches," in *Proc. OFC*, Anaheim, CA, USA, 2006, pp. 1–3, paper PDP25.

[4] E. Kehayas, L. Stampoulidis, H. Avramopoulos, Y. Liu, E. Tangdiongga, and H. J. S. Dorren, "40 Gb/s all-optical packet clock recovery with ultrafast lock-in time and low inter-packet guardbands," *Opt. Express*, vol. 13, no. 2, pp. 475–480, 2005.

[5] X. Tang, J. Cartledge, A. Shen, F. van Dijk, A. Akrout, and G. Duan, "Characterization of all-optical clock recovery for 40 Gb/s RZ-OOK and RZ-DPSK data using mode-locked semiconductor lasers," *J. Lightw. Technol.*, vol. 27, no. 20, pp. 4603–4609, Oct. 15, 2009.

[6] N. Calabretta, *et al.*, "320 Gb/s all-optical clock recovery and time demultiplexing enabled by a single quantum dash mode-locked laser Fabry-Perot optical clock pulse generator," in *Proc. OFC*, Anaheim, CA, USA, Mar. 2013, pp. 1–3, paper OTh4D.5.

[7] G. H. Duan, *et al.*, "High performance InP-based quantum dash semiconductor mode-locked lasers for optical communications," *Bell Labs Tech. J.*, vol. 14, no. 3, pp. 63–84, 2009.

[8] R. Maldonado-Basilio, J. Parra-Cetina, S. Latkowski, N. Calabretta, and P. Landais, "Experimental investigation of the optical injection locking dynamics in single-section quantum-dash Fabry-Pérot laser diode for packet-based clock recovery applications," *J. Lightw. Technol.*, vol. 31, no. 6, pp. 860–865, Mar. 15, 2013.

[9] J. Luo, J. Parra-Cetina, P. Landais, H. J. S. Dorren, and N. Calabretta, "40G burst mode optical clock recovery after 52 km transmission enabled by a dynamically switched quantum dash mode-locked laser," in *Proc. ECOC*, London, U.K., Sep. 2013, pp. 1–3, paper Th.2.A.2.

[10] B. Lavigne, J. Renaudier, F. Lelarge, O. Legouezigou, H. Gariah, and G.-H. Duan, "Polarization-insensitive low timing jitter and highly optical noise tolerant all-optical 40-GHz clock recovery using a bulk and a quantum-dots-based self-pulsating laser cascade," *J. Lightw. Technol.*, vol. 25, no. 1, pp. 170–176, Jan. 2007.

[11] J. Renaudier, G.-H. Duan, P. Landais, and P. Gallion, "Phase correlation and linewidth reduction of 40 GHz self-pulsation in distributed Bragg reflector semiconductor lasers," *IEEE J. Quantum Electron.*, vol. 43, no. 2, pp. 147–156, Feb. 2007.

[12] J. Lasri, P. Devgan, R. Tang, and P. Kumar, "Self-starting optoelectronic oscillator for generating ultra-low-jitter high-rate (10 GHz or higher) optical pulses," *Opt. Express*, vol. 11, no. 12, pp. 1430–1435, 2003.